Research Article | Vol. 29, No. 15 / 19 July 2021 / Optics Express 23421
Optics EXPRESS

Distinguishing monomer and nanoparticle contributions to high-harmonic emission from laser-ablated plumes

JINGGUANG LIANG,[1,2] YU HANG LAI,[1,2,*] WUFENG FU,[1,2] CHUNLEI GUO,[3] AND WEI LI[1,2,4]

[1]GPL, State Key Laboratory of Applied Optics, Changchun Institute of Optics, Fine Mechanics and Physics, Chinese Academy of Sciences, Changchun 130033, China
[2]University of Chinese Academy of Sciences, Beijing 100049, China
[3]The Institute of Optics, University of Rochester, Rochester, NY 14627, USA
[4]weili1@ciomp.ac.cn
[*]laiyh@ciomp.ac.cn

Abstract: Nano-clusters and nano-particles (NPs) are attractive media for high-harmonic generation (HHG) since they combine the advantages of using atomic media (for the low average density) and bulk solid media (for the high local density). Recently, laser ablated plumes from metal nano-powders have been used as HHG media and it has been often assumed that the harmonics mainly come from the NPs in the plumes but not by the isolated atoms/ions. However, this assumption is yet to be fully justified. Here, we show that in fact both NPs and isolated monomers could dominate the harmonic spectrum, depending on which part of the plume is interacting with the driving laser. From the ablated plume of indium NPs, it is found that the harmonic spectra from the region where monomers dominate are distinctively different from the region where NPs dominate. Our results demonstrate that accurately capturing the contribution of NPs in HHG processes requires precise selection of the laser-plasma interaction region, a factor that had not been carefully considered in previous studies.

1. Introduction

High-harmonic generation (HHG) is an attractive route to generate ultrashort coherent extreme ultra-violet pulses [1–13] which have found important applications in ultrafast sciences [4,14,15]. Gas atoms and molecules have been the most common HHG media as they could withstand high laser intensity [3,4,6,10,12,16]. Over the past decade, HHG from solids have also been extensively studied [17–26]. The high density of solids is in principle beneficial for conversion efficiency, but in practice the harmonic yields are severely limited since the driving laser intensity is limited by material damage threshold ($< 10^{13}$ W/cm^2), which is much lower than the typical driving intensities in atomic/molecular HHG experiments ($> 10^{14}$ W/cm^2).

Nano-clusters or nano-particles (NPs) are attractive alternative HHG media since they combine the low average density of gases and local high density of solids which could be beneficial for conversion efficiency. For gaseous species, well-controlled flowing stream of nano-clusters can be produced by supersonic expansion of gas from a nozzle [27–29]. For solid species, however, there is still a lack of robust method for preparing a stream of NPs with sufficient average density for HHG. Although plasma plumes formed by laser ablation from bulk solids may contain NPs [30–36], the concentration is generally low. To generate detectable high harmonics, typically it is required to focus the driving laser at the high-density zone of the plume where lots of monomers (atoms and ions) present and as a result the contribution of NPs (if any) is overwhelmed. To produce ablated plumes rich of NPs, several recent studies used targets composed of nano-powders (see Ref. [37] and the references therein) instead of bulk material. The ablation mechanism for

#428652 https://doi.org/10.1364/OE.428652
Journal © 2021 Received 22 Apr 2021; revised 5 Jun 2021; accepted 5 Jun 2021; published 9 Jul 2021

Optics EXPRESS

such targets has not been elucidated and the spatial-temporal characteristics of the plasma plumes from them remain largely unknown. So far, the only type of indirect evidence which indicates that such plumes contains NPs is the observation that the debris of the ablated matter (collected by a substrate nearby the plume) contains NPs of similar sizes to the original nano-powders [38]. Yet, this type of measurement is not effective for measuring the presence of monomers in the ablated matter and therefore one could not rule out the possibility that the plume composition is still dominated by monomers even with the presence of NPs. Moreover, it is unclear whether the NPs interact with the driving laser effectively, since there has been no clear evidence to show that the arrival time of driving laser coincides with the emission time of the NPs from the sample surface.

Despite these unresolved issues, previous HHG investigations on ablated plumes of NP samples assumed that the harmonic signals are mainly contributed by NPs while the signals from ablated plume of bulk sample are dominated by monomers [38–43]. In some studies, harmonic spectra from the two types of samples show significantly different spectral features [39,41]. But in other studies, the features are less distinguishable even though the overall harmonic intensities are different [38,44]. Although some of the seemingly inconsistent results could be attributed to the difference in the ablation pulse intensity and sample conditions in different experiments, ultimately the inconsistencies might be an indication that the aforementioned assumption is not valid or at least not a good approximation in numerous scenarios.

In this work, we present experimental evidence which suggests that whether the HHG from the ablated plume is contributed by monomers or NPs depends on which part of the plume is interacting with the driving laser. We use indium (In) as the target material, from which the harmonic spectra are featured by a resonance enhanced 13^{th} harmonic [45,46]. The resonant harmonic is treated as a distinctive indicator for the presence of In^+ monomers. By precisely adjusting the lateral distance between the driving laser beam and the ablation surface, we compare the spectra generated from the "head" part (the zone close to the ablation surface) and the "tail" part (the zone far from the ablation surface) of the plasma plume. From the plume ablated from a sample made of In NPs, we observe that, if the lateral distance is sufficiently small, the resonant enhancement disappears. But if the lateral distance is increased, the enhancement resonance revives. This result suggests that HHG from the "head" part of the plume is mainly from NPs while the "tail" part is dominated by monomers. Our investigation could serve as a clear reference for future studies of HHG in NPs from plumes, as it demonstrates the necessity of precise selection of the region for laser-plume interaction for accurately capturing the contribution of NPs in HHG processes.

2. Experimental setup

Our experiments use a 0.8 μm Ti:sapphire laser (Spectra Physics: Spitfire Ace). A 35 fs, 4.5 mJ beam and a 200 ps, 0.5 mJ beam (a split-off from the amplified beam before compression) output from the system are used as the driving pulse (DP) and heating pulse (HP), respectively. The pulse repetition rate is set at 100 Hz. As schematically shown in Fig. 1, the HP is focused on the sample surface by a lens (focal length = 200 mm) for producing a plasma plume. Subsequently, the DP is focused at the plume by a lens of 500 mm focal length. We set up a long optical path for the DP to create a delay between DP and HP. Depending on the path length we set, the delay is either 50 ns or 80 ns.

Two forms of samples are used: In in the form of bulk solid and nanoparticles (NPs) (commercial nano-powders, average diameter 20 nm). The NP sample is prepared by compressing the nano-powders into a tablet with a flat surface. Unlike previous studies where mixture of NPs with polymers (glue) was used as the sample [38,41,47], this method ensures the plasma plume is free of unwanted substances from the polymers. The surface morphology of the NPs sample is shown in the next section.

Optics EXPRESS

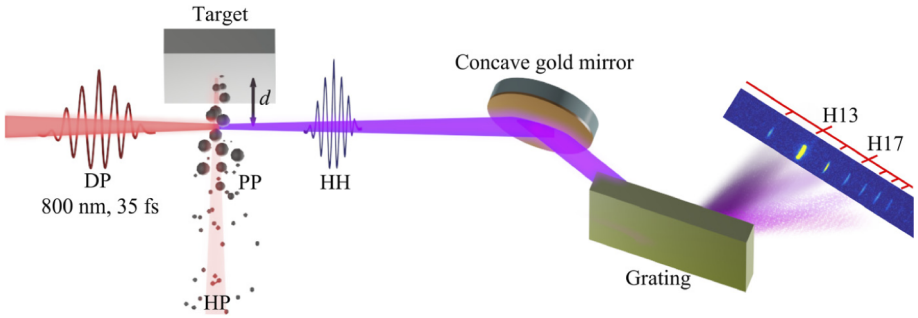

Fig. 1. Schematic setup diagrams. HP: heating pulse; DP: driving pulse; d: distance between target surface and DP; PP: plasma plume; HH: high-harmonics.

Figure 1 shows a schematic diagram of the experimental setup which is inside a vacuum system. The samples are mounted on a three-axis translational stage. The lateral distance d between the sample surface and the DP can be controlled at a precision of 10 μm. The generated harmonics propagate into the back chamber which contains a home-built extreme ultraviolet spectrometer [48], which is composed of concave mirror, a 1200 grooves/mm flat-field grating and a microchannel plate coupled to a phosphor screen. The fluorescence on the screen is captured by a CCD camera. After completion of each harmonic measurement, the sample is translated so that the HP interacts with a fresh surface region in the subsequent measurement.

3. Results and discussion

We first discuss the results from bulk In target. The DP and HP intensities are kept at 3.5×10^{14} W/cm^2 and 1.2×10^{10} W/cm^2, respectively, with a delay of 80 ns. We measure harmonic spectrum as a function of lateral distance d. All the spectra are stacked together and presented as the colour plot in Fig. 2(a). For clarity, two of the selected spectra are plotted in Fig. 2(c): one from a small distance and the other from a large distance (see caption). While the overall harmonic yields decrease as d increases, the yield of the 13th harmonic (H13) is always at least an order of magnitude higher than the neighboring harmonics.

The enhanced harmonic has been explained by the 'four-step' model [49]. The difference between this model and the commonly used 'three-step' model for HHG is that the returning electron recombines to an autoionizing state and then relaxes to the ground state, instead of directly recombining to ground state. For example from In plasma, the enhanced harmonic is a result of the resonant transition between the two states in In^+ ion: $4d^95s^25p(^2D)^1P_1 \rightarrow 4d^{10}5s^2\ ^1S_0$ [45]. The energy of this transition is 19.92 eV, which is very close to the photon energy of H13 driven by 0.8 μm laser. An important remark here is that this model is based on an isolated single ion and it is in fact unlikely that such resonance process could play a similar role in the HHG process in an NP because (i) the electronic states of an isolated atom and a group of closely bounded atoms can be very different, and (ii) electron ionization and recombination process in an NP could involve multiple atoms.

The results of bulk In indicate that the harmonics are mainly generated from In^+ ions, and the distribution of the ion density is essentially a monotonic function of the distance. On the other hand, however, results from NP target are more intriguing. The data are shown in Figs. 2(b) and 2(d), where the experimental conditions are same as that of bulk In. The spectra generated from near region and far region are distinctively different. At small distances ($d < 150$ μm), the spectra are essentially featureless without resonant enhancement, although the overall yields vary as a function of distance. For large distances ($d > 150$ μm), however, the spectra resemble the case of bulk In with strong H13. For clarity, Fig. 3(a) shows the yield of H13 as a function of distance

Optics EXPRESS

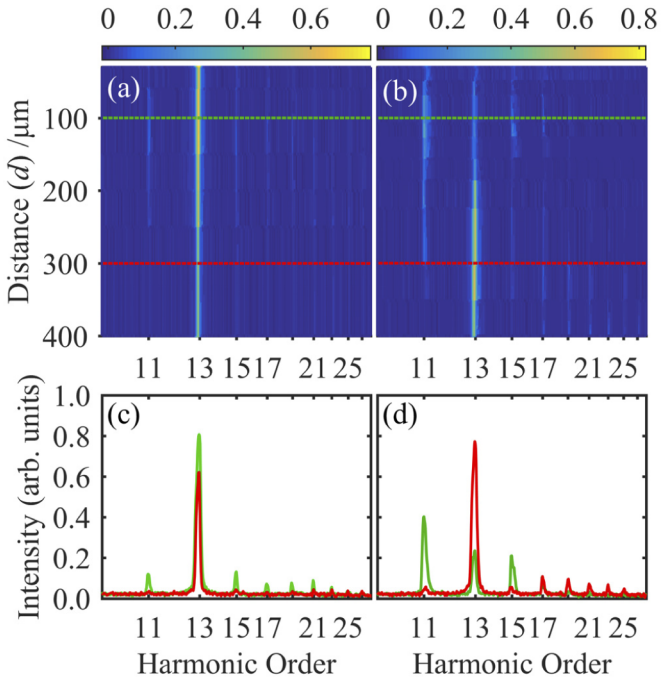

Fig. 2. (a) Harmonic spectra from the plasma plume of bulk target *vs d*. (b) Same as (a) but for nanoparticles target. (c) Spectra in (a) at two selected lateral distances (green: 100 μm; red: 300 μm). (d) Spectra in (b) at two selected lateral distances (green: 100 μm; red: 300 μm).

(red dots). It is quite weak at small distances and grow upto maximum when the $d \approx 200$–300 μm. As a comparison of two regions, we show the distance dependence of H11 in Fig. 3(b) (red). H11 is selected because it is the strongest harmonic from the near region. In contrast to H13, the distribution is peaked at a small distance (~ 100 μm), as indicated by the vertical red dashed line.

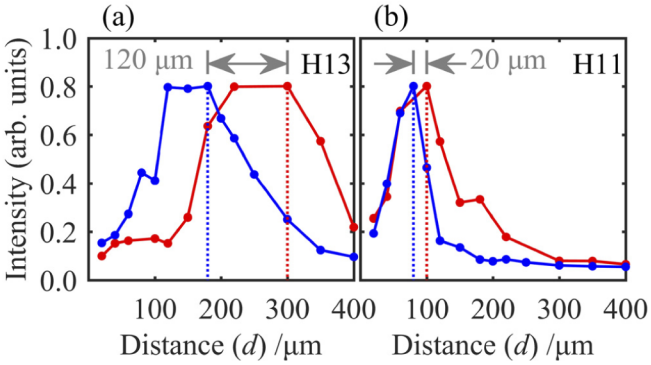

Fig. 3. (a) H13 and (b) H11 intensities from the plasma plume of indium nanoparticles as a function of the lateral distance *d*. Red: 80 ns delay; blue: 50 ns delay.

These results suggest that the plume of NPs seems to have two distinctive zones dominated by different substances. To probe the temporal evolution of the two groups of substances, we repeat the distance dependent measurements at a different HP-DP delay (50 ns). Again, we extract the distance dependence of H13 and H11 and they are plotted in Fig. 3 (blue) together with the

Optics EXPRESS

corresponding results at 80 ns delay. For both harmonic orders, the distributions in the case of 50 ns are peaked at smaller distances relative to the results at 80 ns. This is a direct indication that the peak positions correspond to two groups of ablated substances moving outward at different velocities. From the shift of the peak positions divided by the time differences, the velocities of the two groups of components are calculated to be around 670 m/s and 4000 m/s. Such difference in velocity [50,51] seems to suggest that for plumes of NP samples, the dominate particles at near distances are large size clusters or NPs, while for the far distances are small size ions.

While it is clear that the "fast" group contains In^+ monomers, more concrete evidence is needed to justify that the "slow" group indeed contains NPs. Although the absence of the enhanced H13 from the "slow" group strongly suggests that there is a lack of In^+ monomers, one may argue that the featureless harmonic spectrum might not necessarily be due to NPs, instead it could be due to neutral In monomers. Here we present two evidences to support our conjecture that HHG from the "slow" group are contributed by NPs.

The first evidence is based on neutral depletion due to ionization. Neutral In atom has a very low ionization potential (5.79 eV), so it is readily ionized. Strong-field ionization (using the PPT model [52]) calculations indicate that the ionization probability saturates at an intensity ($<10^{13}$ W/cm^2) much lower than our experimental value. Therefore, if an In atom is irradiated by our DP, it is highly probable to be ionized rapidly while it is just interacting with the rising edge of the pulse. Subsequently, the central intense part of the DP would interact with the pre-formed In^+ ion, which should then lead to the generation of the resonant H13. From the argument above, we anticipate that the resonant H13 should appear even if the medium only contains neutral atoms, as long as the DP intensity is sufficiently high. Note that the same argument could not be necessarily applied to NP, since it is unlikely that resonant harmonic could be generated from NP at all, as we explained previously.

To confirm that the DP intensity is not a factor for the absence of the resonant H13, we carry out harmonic measurements at two different DP intensities, 1.6×10^{14} W/cm^2 and 5.9×10^{14} W/cm^2 (lower and higher than the intensity at Fig. 2, respectively). Here we keep $d \approx 80$ μm and the HP-DP delay at 80 ns. The spectra from bulk In and NPs targets are shown in Figs. 4(a) and 4(b), respectively. For bulk In, the presence of the resonant H13 is independent of the DP intensity, as expected. On the other hand, the absence of the resonant H13 from NPs also appears to be independent of the DP intensity. Increasing the DP intensity only lead to an overall yields increase and a cut-off energy extension of the cutoff energy. Therefore, this result helps us to rule out the contribution due to neutral In monomers.

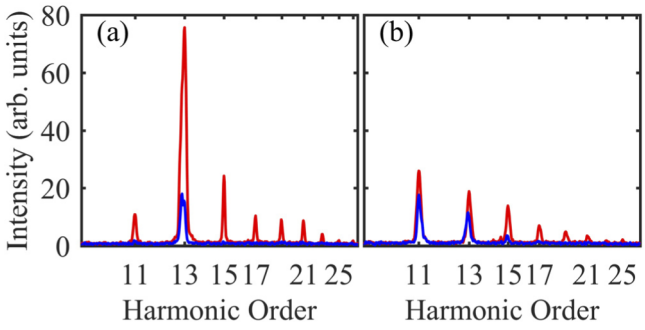

Fig. 4. Harmonic spectra generated from the plasma plume of In (a) bulk and (b) nanoparticles target at low (blue, 1.6×10^{14} W/cm^2) and high (red, 5.9×10^{14} W/cm^2) DP intensity.

The second evidence is based on measurements of laser power attenuation due to the plasma plumes [53]. We put a detector behind the plasma plume to measure the power loss of the DP

Optics EXPRESS

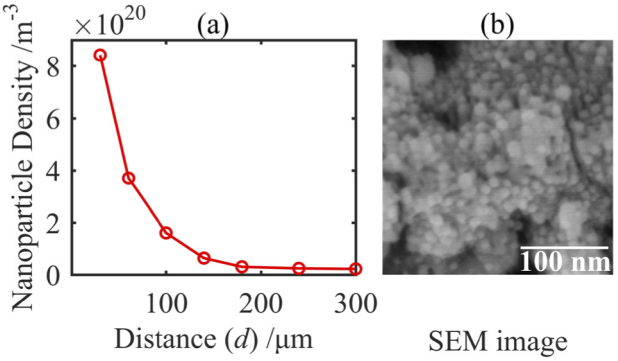

Fig. 5. (a) Calculated nanoparticle density as a function of d. (b) Surface morphology of the indium nanoparticles target after laser ablation.

due to its passage through the plume. We use a weak DP whose intensity is about two orders of magnitude weaker than that used in HHG experiments to ensure that the measured attenuation (if any) is not originated from nonlinear processes. The HP-DP delay is set at 80 ns.

Attenuation is determined by comparing the laser power without and with the presence of the plume (P_0 and P_1). Due to the limited sensitivity of this measurement, the HP intensity used here (6.1×10^{10} W/cm^2) is higher than that in HHG experiments, so as to make a higher NP density. For bulk In, the two power values are essentially same within the inherent power fluctuation of the laser itself, implying no attenuation. This indicates that In monomers (atoms or ions) are ineffective absorbers or scatterers for 0.8 μm laser, as expected.

On the other hand, the attenuation in the case of In NPs is significant, which is a clear indication of the presence of NPs in the plasma plume. For $d < 50$ μm, the DP is attenuated by up to 30%. Without having to consider nonlinear absorption, the attenuation could be modelled simply using the Rayleigh scattering theory for small particles together with Beer's law: $P_1/P_0 = 1 - e^{-(Q_{SCA}+Q_{ABS})\pi r^2 N z}$ [53], where r is the particle radius, N is the particle density, z is the laser-particle interaction length, Q_{SCA} and Q_{ABS} are the efficiency term and the absorption term in the Rayleigh scattering formula, respectively. These two terms are readily calculated by using the value of the complex refractive index of In solid. We set r = 20 nm, which is the average value of the NPs. Figure 5(b) shows a SEM image of the ablated surface of the NPs sample.

We perform the attenuation measurement as a function of distance and use the equation above to estimate the NP density. The results are plotted in Fig. 5(a), it is found that the distribution decays to near-zero at about 150 μm, similar to the distance where harmonic signals vanishes from the "slow" group, as shown in Fig. 3(b). Since the HP intensity used here is higher than that in the HHG experiments, it is likely that the NPs velocities here is higher. However, we believe that the increases in velocities are not drastic. It is because in the distance dependent HHG experiment, we find that if the HP intensity is increased from 1.2 to 4.3×10^{10} W/cm^2, the peak positions of the harmonic distributions for H11 and H13 are shifted up by only ~30% or less. Regardless, neither the HHG nor attenuation measurements could be treated as a precise way to actually probe the velocities distribution of the NPs, rather they could only be treated as evidence which indicate that NPs indeed exist in the plasma. Obtaining a complete spatial-temporal distribution of the plasma plumes require more demanding techniques such as time-resolved optical emission spectroscopy [54] or x-ray-absorption fine structure imaging [55], which is beyond the scope of our study. Nevertheless, our results have already provided clear evidence to reveal the contributions of NPs and monomer ions in the HHG process.

Although there is a lack of studies on the ablation mechanisms for nano-powders targets, it is reasonable to anticipate that the process of NPs emission is very different from the case of bulk

Optics EXPRESS

metal. For ablation of bulk metal, the formation of NPs involves ultrafast heating, expansion and phase transition which are rather complex and require the HP to be in a specific intensity and pulse duration ranges, therefore the number of NPs in the plumes are limited. On the other hand, the emission process of NPs from a sample composed of NPs should be more direct, since all the NPs are "pre-formed" and they are held together just by friction. Therefore, they are easily removed from the sample surface upon laser irradiation. Nevertheless, although this kind of plasma plume contain sufficient number of NPs for HHG, the contribution of monomers can still be very significant and could not be overlooked, as we have demonstrated.

4. Conclusion

In conclusion, we show that, from the laser ablated plume of In nano-powders, there exist two zones where the high-harmonics are generated by the monomers and NPs, respectively. The zone far away from the ablation surface gives the resonant H13 which is a signature of the isolated In^+ ions; the zone close to the ablation surface gives a "featureless" spectrum by the NPs. The existence of NPs in the plume is confirmed by attenuation measurements. Our results demonstrate that accurately distinguishing the contribution of NPs from that of monomers in HHG processes requires precise selection of the laser-plasma interaction region, a factor which was essentially overlooked in previous studies.

Funding. National Natural Science Foundation of China (12004380); Jilin Scientific and Technological Development Program (YDZJ202102CXJD002).

Acknowledgments. Y.H. Lai acknowledges discussions with Professor Pierre Agostini.

Disclosures. The authors declare no competing financial interest.

Data availability. Data underlying the results presented in this paper are not publicly available at this time but may be obtained from the authors upon reasonable request.

References

1. M. Hentschel, R. Kienberger, C. Spielmann, G. A. Reider, N. Milosevic, T. Brabec, P. Corkum, U. Heinzmann, M. Drescher, and F. Krausz, "Attosecond metrology," Nature **414**(6863), 509–513 (2001).
2. A. Rundquist, C. G. Durfee, Z. Chang, C. Herne, S. Backus, M. M. Murnane, and H. C. Kapteyn, "Phase-matched generation of coherent soft X-rays," Science **280**(5368), 1412–1415 (1998).
3. P.-M. Paul, E. S. Toma, P. Breger, G. Mullot, F. Augé, P. Balcou, H. G. Muller, and P. Agostini, "Observation of a train of attosecond pulses from high harmonic generation," Science **292**(5522), 1689–1692 (2001).
4. T. Popmintchev, M.-C. Chen, P. Arpin, M. M. Murnane, and H. C. Kapteyn, "The attosecond nonlinear optics of bright coherent X-ray generation," Nat. Photonics **4**(12), 822–832 (2010).
5. C. Jin, G. J. Stein, K.-H. Hong, and C. D. Lin, "Generation of bright, spatially coherent soft X-ray high harmonics in a hollow waveguide using two-color synthesized laser pulses," Phys. Rev. Lett. **115**(4), 043901 (2015).
6. S. M. Teichmann, F. Silva, S. Cousin, M. Hemmer, and J. Biegert, "0.5-keV Soft X-ray attosecond continua," Nat. Commun. **7**(1), 11493–6 (2016).
7. Y. Pan, F. Guo, C. Jin, Y. Yang, and D. Ding, "Selection of electron quantum trajectories in the macroscopic high-order harmonics generated by near-infrared lasers," Phys. Rev. A **99**(3), 033411 (2019).
8. Y. Pertot, C. Schmidt, M. Matthews, A. Chauvet, M. Huppert, V. Svoboda, A. von Conta, A. Tehlar, D. Baykusheva, and J.-P. Wolf, "Time-resolved x-ray absorption spectroscopy with a water window high-harmonic source," Science **355**(6322), 264–267 (2017).
9. H. W. Sun, P. C. Huang, Y. H. Tzeng, J. T. Huang, C. D. Lin, C. Jin, and M. C. Chen, "Extended phase matching of high harmonic generation by plasma-induced defocusing," Optica **4**(8), 976–981 (2017).
10. M. Ferray, A. L'Huillier, X. Li, L. Lompre, G. Mainfray, and C. Manus, "Multiple-harmonic conversion of 1988 nm radiation in rare gases," J. Phys. B: At., Mol. Opt. Phys. **21**(3), L31–L35 (1988).
11. N. Kanda, T. Imahoko, K. Yoshida, A. Tanabashi, A. A. Eilanlou, Y. Nabekawa, T. Sumiyoshi, M. Kuwata-Gonokami, and K. Midorikawa, "Opening a new route to multiport coherent XUV sources via intracavity high-order harmonic generation," Light: Sci. Appl. **9**(1), 168–169 (2020).
12. A. McPherson, G. Gibson, H. Jara, U. Johann, T. S. Luk, I. McIntyre, K. Boyer, and C. K. Rhodes, "Studies of multiphoton production of vacuum-ultraviolet radiation in the rare gases," J. Opt. Soc. Am. B **4**(4), 595–601 (1987).
13. M. Gebhardt, T. Heuermann, R. Klas, C. Liu, A. Kirsche, M. Lenski, Z. Wang, C. Gaida, J. Antonio-Lopez, and A. Schülzgen, "Bright, high-repetition-rate water window soft X-ray source enabled by nonlinear pulse self-compression in an antiresonant hollow-core fibre," Light: Sci. Appl. **10**(1), 36–37 (2021).

Optics EXPRESS

14. C. Winterfeldt, C. Spielmann, and G. Gerber, "Colloquium: Optimal control of high-harmonic generation," Rev. Mod. Phys. **80**(1), 117–140 (2008).
15. F. Krausz and M. Ivanov, "Attosecond physics," Rev. Mod. Phys. **81**(1), 163–234 (2009).
16. Q. Gao, S. Chen, H. Liang, Y. Wang, C. Bi, S. Ben, R. Ma, D. Ding, and J. Chen, "Comparison study on atomic and molecular ellipticity dependence of high-order harmonic generation," Phys. Rev. A **103**(4), 043115 (2021).
17. S. Ghimire, A. D. DiChiara, E. Sistrunk, P. Agostini, L. F. DiMauro, and D. A. Reis, "Observation of high-order harmonic generation in a bulk crystal," Nat. Phys. **7**(2), 138–141 (2011).
18. O. Schubert, M. Hohenleutner, F. Langer, B. Urbanek, C. Lange, U. Huttner, D. Golde, T. Meier, M. Kira, and S. W. Koch, "Sub-cycle control of terahertz high-harmonic generation by dynamical Bloch oscillations," Nat. Photonics **8**(2), 119–123 (2014).
19. T. T. Luu, M. Garg, S. Y. Kruchinin, A. Moulet, M. T. Hassan, and E. Goulielmakis, "Extreme ultraviolet high-harmonic spectroscopy of solids," Nature **521**(7553), 498–502 (2015).
20. G. Vampa, T. Hammond, N. Thiré, B. Schmidt, F. Légaré, C. McDonald, T. Brabec, and P. Corkum, "Linking high harmonics from gases and solids," Nature **522**(7557), 462–464 (2015).
21. G. Ndabashimiye, S. Ghimire, M. Wu, D. A. Browne, K. J. Schafer, M. B. Gaarde, and D. A. Reis, "Solid-state harmonics beyond the atomic limit," Nature **534**(7608), 520–523 (2016).
22. H. Kim, S. Han, Y. W. Kim, S. Kim, and S.-W. Kim, "Generation of coherent extreme-ultraviolet radiation from bulk sapphire crystal," ACS Photonics **4**(7), 1627–1632 (2017).
23. K. Kaneshima, Y. Shinohara, K. Takeuchi, N. Ishii, K. Imasaka, T. Kaji, S. Ashihara, K. L. Ishikawa, and J. Itatani, "Polarization-resolved study of high harmonics from bulk semiconductors," Phys. Rev. Lett. **120**(24), 243903 (2018).
24. Y. W. Kim, T.-J. Shao, H. Kim, S. Han, S. Kim, M. Ciappina, X.-B. Bian, and S.-W. Kim, "Spectral interference in high harmonic generation from solids," ACS Photonics **6**(4), 851–857 (2019).
25. N. Klemke, N. Tancogne-Dejean, G. M. Rossi, Y. Yang, F. Scheiba, R. Mainz, G. Di Sciacca, A. Rubio, F. Kärtner, and O. Mücke, "Polarization-state-resolved high-harmonic spectroscopy of solids," Nat. Commun. **10**(1), 1319–1327 (2019).
26. J. Li, J. Lu, A. Chew, S. Han, J. Li, Y. Wu, H. Wang, S. Ghimire, and Z. Chang, "Attosecond science based on high harmonic generation from gases and solids," Nat. Commun. **11**(1), 1–13 (2020).
27. J. Tisch, T. Ditmire, D. Fraser, N. Hay, M. Mason, E. Springate, J. Marangos, and M. Hutchinson, "Investigation of high-harmonic generation from xenon atom clusters," J. Phys. B: At., Mol. Opt. Phys. **30**(20), L709–L714 (1997).
28. C. Vozzi, M. Nisoli, J. Caumes, G. Sansone, S. Stagira, S. De Silvestri, M. Vecchiocattivi, D. Bassi, M. Pascolini, and L. Poletto, "Cluster effects in high-order harmonics generated by ultrashort light pulses," Appl. Phys. Lett. **86**(11), 111121 (2005).
29. H. Ruf, C. Handschin, R. Cireasa, N. Thiré, A. Ferré, S. Petit, D. Descamps, E. Mével, E. Constant, and V. Blanchet, "Inhomogeneous high harmonic generation in krypton clusters," Phys. Rev. Lett. **110**(8), 083902 (2013).
30. W. Marine, L. Patrone, B. Luk'yanchuk, and M. Sentis, "Strategy of nanocluster and nanostructure synthesis by conventional pulsed laser ablation," Appl. Surf. Sci. **154-155**, 345–352 (2000).
31. D. Perez and L. J. Lewis, "Molecular-dynamics study of ablation of solids under femtosecond laser pulses," Phys. Rev. B **67**(18), 184102 (2003).
32. S. Amoruso, G. Ausanio, A. Barone, R. Bruzzese, L. Gragnaniello, M. Vitiello, and X. Wang, "Ultrashort laser ablation of solid matter in vacuum: a comparison between the picosecond and femtosecond regimes," J. Phys. B: At., Mol. Opt. Phys. **38**(20), L329–L338 (2005).
33. S. Amoruso, G. Ausanio, R. Bruzzese, M. Vitiello, and X. Wang, "Femtosecond laser pulse irradiation of solid targets as a general route to nanoparticle formation in a vacuum," Phys. Rev. B **71**(3), 033406 (2005).
34. D. Scuderi, O. Albert, D. Moreau, P. Pronko, and J. Etchepare, "Interaction of a laser-produced plume with a second time delayed femtosecond pulse," Appl. Phys. Lett. **86**(7), 071502 (2005).
35. S. Noël, J. Hermann, and T. Itina, "Investigation of nanoparticle generation during femtosecond laser ablation of metals," Appl. Surf. Sci. **253**(15), 6310–6315 (2007).
36. J. Perrière, C. Boulmer-Leborgne, R. Benzerga, and S. Tricot, "Nanoparticle formation by femtosecond laser ablation," J. Phys. D: Appl. Phys. **40**(22), 7069–7076 (2007).
37. R. Ganeev, "Enhancement of high-order harmonics generated in laser-produced plasma using ionic resonances and nanoparticles," Opt. Spectrosc. **122**(2), 250–268 (2017).
38. H. Singhal, R. Ganeev, P. Naik, A. Srivastava, A. Singh, R. Chari, R. Khan, J. Chakera, and P. Gupta, "Study of high-order harmonic generation from nanoparticles," J. Phys. B: At., Mol. Opt. Phys. **43**(2), 025603 (2010).
39. R. Ganeev, L. E. Bom, and T. Ozaki, "Application of nanoparticle-containing laser plasmas for optical harmonic generation," J. Appl. Phys. **106**(2), 023104 (2009).
40. L. Elouga Bom, R. Ganeev, J. Abdul-Hadi, F. Vidal, and T. Ozaki, "Intense multimicrojoule high-order harmonics generated from neutral atoms of In 2 O 3 nanoparticles," Appl. Phys. Lett. **94**(11), 111108 (2009).
41. T. Ozaki, L. E. Bom, J. Abdul-Hadi, and R. Ganeev, "Evidence of strong contribution from neutral atoms in intense harmonic generation from nanoparticles," Laser Part. Beams **28**(1), 69–74 (2010).
42. R. Ganeev, M. Suzuki, S. Yoneya, and H. Kuroda, "Resonance-enhanced harmonic generation in nanoparticle-containing plasmas," J. Phys. B: At., Mol. Opt. Phys. **48**(16), 165401 (2015).

Optics EXPRESS

43. M. Venkatesh, R. A. Ganeev, D. S. Ivanov, G. S. Boltaev, V. V. Kim, J. Liang, A. A. Samokhvalov, A. V. Kabashin, S. M. Klimentov, and M. E. Garcia, "High-Order Harmonic Generation in Au Nanoparticle-Contained Plasmas," Nanomaterials **10**(2), 234 (2020).
44. R. Ganeev, "High-order harmonic generation in nanoparticle-containing laser-produced plasmas," Laser Phys. **18**(9), 1009–1015 (2008).
45. R. A. Ganeev, M. Suzuki, M. Baba, H. Kuroda, and T. Ozaki, "Strong resonance enhancement of a single harmonic generated in the extreme ultraviolet range," Opt. Lett. **31**(11), 1699–1701 (2006).
46. Z. Abdelrahman, M. Khokhlova, D. Walke, T. Witting, A. Zair, V. Strelkov, J. Marangos, and J. Tisch, "Chirp-control of resonant high-order harmonic generation in indium ablation plumes driven by intense few-cycle laser pulses," Opt. Express **26**(12), 15745–15758 (2018).
47. R. Ganeev, M. Suzuki, M. Baba, M. Ichihara, and H. Kuroda, "High-order harmonic generation in Ag nanoparticle-containing plasma," J. Phys. B: At., Mol. Opt. Phys. **41**(4), 045603 (2008).
48. J. Liang, M. Venkatesh, G. S. Boltaev, R. A. Ganeev, Y. H. Lai, and C. Guo, "Investigation of Resonance-Enhanced High-Order Harmonics by Two-Component Laser-Produced Plasmas," Atoms **9**(1), 1 (2021).
49. V. Strelkov, "Role of autoionizing state in resonant high-order harmonic generation and attosecond pulse production," Phys. Rev. Lett. **104**(12), 123901 (2010).
50. S. Amoruso, R. Bruzzese, N. Spinelli, R. Velotta, M. Vitiello, and X. Wang, "Emission of nanoparticles during ultrashort laser irradiation of silicon targets," Europhys. Lett. **67**(3), 404–410 (2004).
51. S. Amoruso, R. Bruzzese, N. Spinelli, R. Velotta, M. Vitiello, X. Wang, G. Ausanio, V. Iannotti, and L. Lanotte, "Generation of silicon nanoparticles via femtosecond laser ablation in vacuum," Appl. Phys. Lett. **84**(22), 4502–4504 (2004).
52. A. Perelomov, V. Popov, and M. Terent'ev, "Ionization of atoms in an alternating electric field," Sov. Phys. JETP **23**, 924–934 (1966).
53. J. Greses, P. Hilton, C. Barlow, and W. Steen, "Plume attenuation under high power Nd: yttritium–aluminum–garnet laser welding," J. Laser Appl. **16**(1), 9–15 (2004).
54. P. Sankar, J. J. Nivas, N. Smijesh, G. K. Tiwari, and R. Philip, "Optical emission and dynamics of aluminum plasmas produced by ultrashort and short laser pulses," J. Anal. At. Spectrom. **32**(6), 1177–1185 (2017).
55. K. Oguri, Y. Okano, T. Nishikawa, and H. Nakano, "Dynamics of femtosecond laser ablation studied with time-resolved x-ray absorption fine structure imaging," Phys. Rev. B **79**(14), 144106 (2009).